

ASPERA ELS UV SUPPRESSION STUDY FINAL REPORT

D. C. SLATER
SOUTHWEST RESEARCH INSTITUTE

I. INTRODUCTION

The ASPERA ELS instrument must incorporate an adequate light baffle design to preclude solar UV photons that enter the instrument from making their way to the MCP detector via multiple reflections within its interior housing. In particular, the MCPs are sensitive to the strong H-Ly α emission at 1216 Å emitted by the Sun (at 1 AU the solar flux at this wavelength is $\sim 2.4 \times 10^{11}$ photons $\text{cm}^{-2} \text{s}^{-1}$), which, if stimulated by these photons will create a significant detector background rate. In addition, any photoelectrons created by these photons inside the instrument must also be rejected via electrostatic repeller grids placed over the MCP detector. In order to achieve a low background rate output from the detector of $\sim 1\text{-}2 \text{ s}^{-1}$, it is necessary that the UV light suppression be $< 10^{-10}$ (assumes an input entrance aperture of $\sim 4.52 \text{ cm}^2$ for the ELS instrument, and a detective quantum efficiency [DQE] for the detector of ~ 0.03 at H-Ly α —a common DQE value for bare MCPs at this wavelength).

The ASPERA ELS design, shown in cross section in Figure 1, is composed of the following sections that were modeled with a non-sequential ray tracing program: a) the top hat; b) the inner and outer deflection plates; and c) the MCP detector. The non-sequential ray tracing program used in this study was ASAPTM (version 6.5) by Breault Research Organization, Inc. A set of evenly spaced light baffles were modeled in the top hat section along with a set of light trap baffles in the top portion of the outer deflection plate. The top hat baffles are the “first line of defense” in preventing photons from entering the curved deflection plate section where the two closely spaced spherical plates act as a waveguide in directing photons to the MCP detector. The second and final line of defense against photons that get to the deflection plates are the set of baffles placed in the upper region of the outer spherical deflection plate. These baffles act as 1) light traps (i.e. trapping photons within their long linear cavities), and 2) light deflectors (with proper design) causing entering photons to reflect back towards the entrance aperture of the instrument. The name of the game is to ensure that the overall baffle design causes photons entering the instrument to a) be rejected (i.e. to reflect back through the entrance aperture into space); and/or b) make a sufficiently large number of internal reflections within the instrument so that by the time they reach the MCP detector they are effectively extinguished via absorption with the blackened walls and baffle surfaces inside the housing (e.g. an internal wall reflection of $\sim 10\%$ would require a minimum of 8 reflections before reaching the MCP detector surface to achieve a photon rejection ratio of 10^8).

The top hat baffle design shown in Figure 1 was found to be more than adequate to preclude any portion of the inner opening of the top hat from having a direct view of the top and bottom wall surfaces to which these baffles are attached. The effect of multiple reflections within the top hat section in allowing rays to enter the spherical deflection plate region (and eventual propagation to the MCP detector), however, required propagating rays through the total modeled system. This was accomplished with a set of 5 different outer deflection plate baffle designs. The results of these ray tracing runs are presented in the remainder of this report. The most optimum of the 5 modeled designs was found to suppress UV photons from reaching the MCP detector by a factor of $< 10^{-10}$, assuming that all the interior surfaces have a UV reflectivity of < 0.2 (preferably < 0.1 at 1216 Å), which should be easily accomplished with blackened coatings such as CuO ⁽¹⁾.

¹ Scott, S., C. Alsop, and L. Free, *Measurement Techniques in Space Plasmas: Particles*, Geophysical Monograph 102, pp. 269-274, 1998.

II. OUTER DEFLECTION PLATE BAFFLE DESIGN/RAY TRACE RESULTS

A. Baffle Design Parameters

Five different outer plate baffle designs were first ray-traced to determine which provided the highest suppression of light entering the deflector plate region from reaching the detector. These five outer plate baffle designs are shown in Figure 2; Table I tabulates the design parameters (i.e. number of baffles, spacing, and baffle openings) for each design. Note that the first outer baffle design (designated OBD1) has spherically curved surfaces that span each baffle opening. These spherical surfaces have a single radius that matches the radius of the outer deflection plate. Because of the concern in fabricating this set of complicated baffles within the outer plate, the remaining four baffle designs studied (OBD2-5) had straight (flat) vertical walls that separated the baffle openings, which could be more easily fabricated by stacking up a set of plates with different circular cut openings. The design parameters were varied in each of these remaining OBDs to ascertain their effects on light suppression. The lower vertex of each OBD2-5 was constrained to fall on the outer deflection plate's spherical radius, projected from the center of the outer deflection plate's spherical surface (see Figure 3). This geometry presumably, minimizes distortions to the electric field in this region when the required voltages are applied to the inner and outer deflection plates during instrument operation (OBD1 has a less evasive effect to this E-field due to the spherically curved outer wall surfaces between baffle openings).

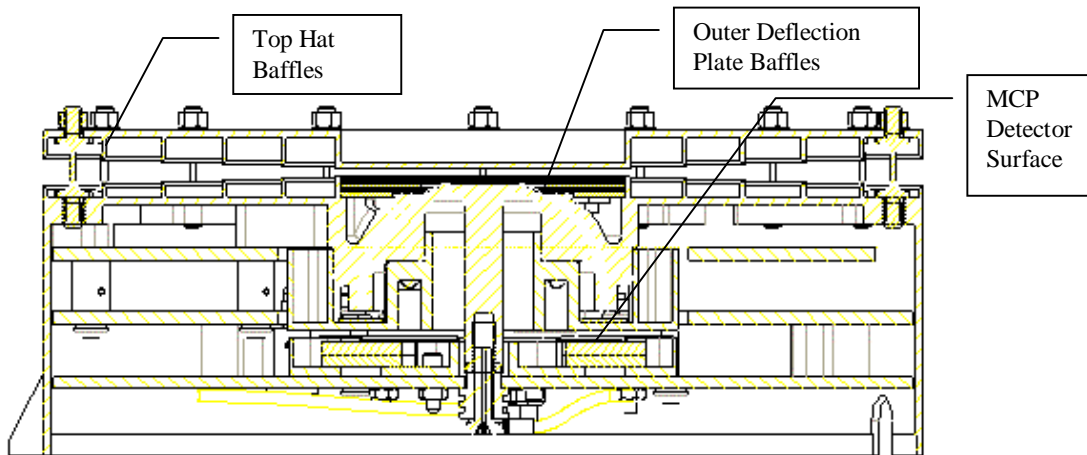


Figure 1. Cross sectional view of the Aspera ELS design. Light suppression baffles are located in a) the top hat section; and b) in the top portion of the outer deflection plate. This design (with variations in the outer deflection plate baffles) was ray traced to quantify its light suppression performance.

To speed up coding each baffle design model in ASAP, two IDL programs were written that computed the necessary baffle shape endpoints based on user specified design parameter inputs (same as in Table I)². The output of this program was then pasted into the ASAP model file for the entire instrument structure. Check runs were conducted to insure the design was properly coded.

TABLE I. Outer Plate Light Baffle Design Parameters					
Baffle Design	Outer Wall Shape	Number of Openings	Baffle Opening	Baffle Spacing	Baffle Length
OBD1	Spherical	5	0.005"	0.005"	0.100 "
OBD2	Flat	5	0.005"	0.010"	0.585"
OBD3	Flat	5	0.005"	0.010"	0.450"
OBD4	Flat	5	0.010"	0.005"	0.585"
OBD5	Flat	10	0.005"	0.005"	0.585"

² Aspera.pro computes the endpoints for the spherically curved baffle wall design; Aspera2.pro computes the endpoints for the flat surfaced wall design.

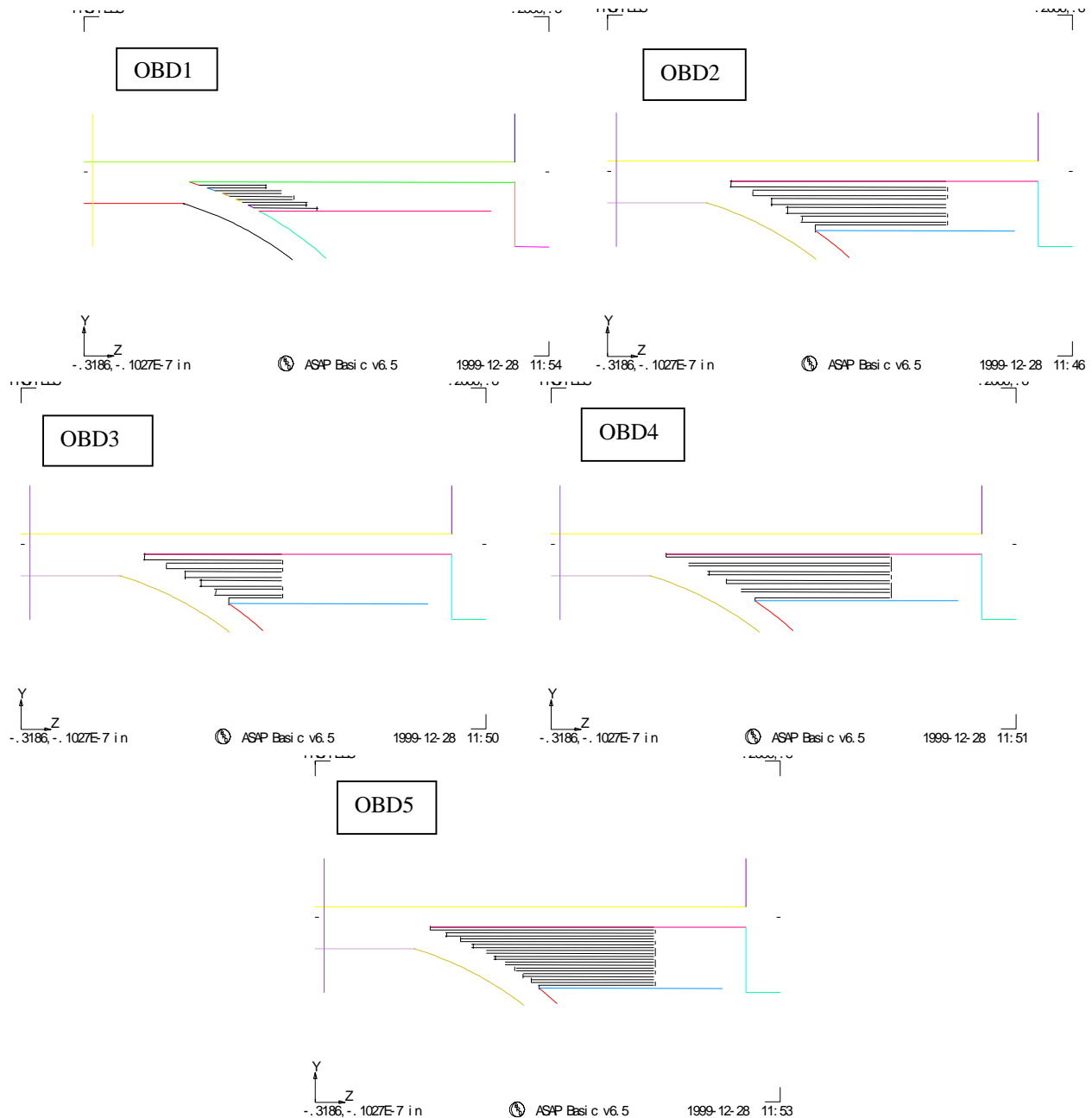


Figure 2. Profile schematics showing each OBD design. Note that these ASAP graphics show some discontinuities that in reality (and as far as the ray tracing is concerned) do not exist.

B. Ray Trace Results

For each OBD, a 10 x 10 grid (100 rays) of collimated rays spanning a rectangular area of 0.001" x 0.001" was placed at the center of the top hat structure of the instrument and propagated towards the gap between the inner and outer deflection plates with a single propagation direction. Twenty-one propagation directions with different elevation angles were traced between 6° and 15° at 0.5° intervals (the azimuthal angle was fixed at 0° for all starting rays). This angular interval spanned rays from the center of the instrument to the entire baffle region (see Figure 4). To speed up the traces and to ensure that a measurable amount of flux reached the MCP detector (a normalized flux ratio—output to input—of $>10^{-13}$), a reflectivity of 0.9 for all surfaces was input to the model. All surfaces were modeled to reflect as a specular surface (again to speed up the runs).

The normalized flux reaching the MCP detector as a function of the input elevation angle from the center of the top hat section of the instrument is shown in Figures 5-8. A large variation in flux reaching the detector is evident from these plots with elevation angle (between $\sim 10^{-13}$ and $< \sim 1$). This variation is expected since certain angles are expected that either a) cause most rays to get trapped within the baffles, b) cause most rays to leave the deflector plate region, or c) allow rays to easily reach the detector because rays do not initially enter any baffle opening, and

the walls allow a direct bouncing pass to the detector with a minimum number of bounces.

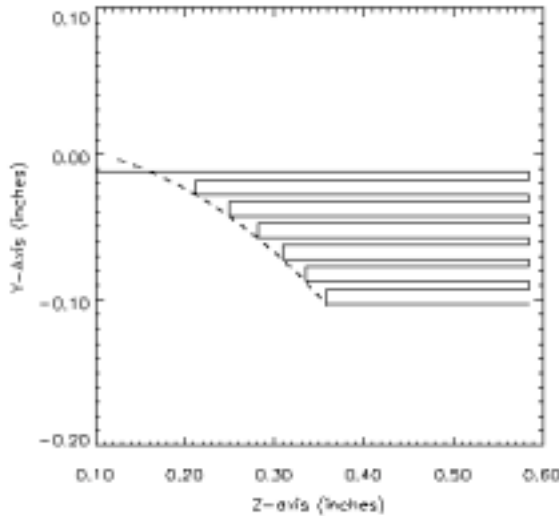


Figure 3. Plot showing the profile of OBD2. The dashed line is an extension of the outer deflector plate sphere showing where the lower left corner of each baffle is positioned. The vertical scale in this plot is magnified by a factor of 1.7 over the horizontal scale to more easily show the baffle structure.

The most critical parameter that affects UV light suppression is the shape of the outer wall. Note that OBD1 has the poorest (i.e. the highest) flux ratio across most of the elevation input angles. Most of the photons that bounce between the baffle openings are reflected downward towards the detector (see Figure 9). Only those angles that allow the photon to enter the baffle opening are trapped. All the remaining OBDs (2-5) showed higher light suppression due to the fact that the flat wall surface between baffle openings had the effect of reflecting most rays striking these surfaces back towards where the rays originated and in some cases out to the outer baffles in the top hat section of the instrument (see Figure 10).

baffle openings. When this occurred (see Figure 11), the photons made more than 20 bounces before reaching the detector. With a wall reflectivity of $\sim 10\%$, the flux reaching the detector would be $< 10^{-20}$! Indeed, the baffles at the top of the outer deflection plate greatly improve the UV light suppression of the instrument.

The lowest flux reaching the MCP detector generally occurred when the photons were trapped within one or more

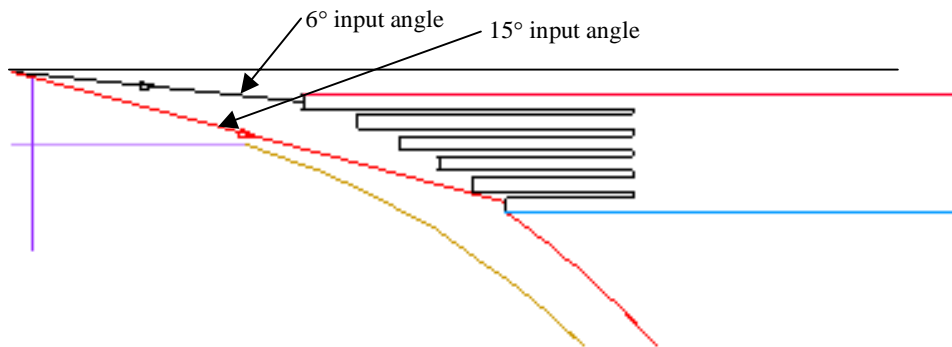


Figure 4. Plot showing angle of incidence for rays directed towards the baffle section in the outer deflection plate. The input angle is measured with respect to the horizontal (z-axis).

The best of the five outer plate baffle designs in suppressing light to the detector is sort of a toss up between OBD4 and OBD5, with OBD5 slightly better (based on the number of elevation input angles that gave lower normalized flux ratios that reached the detector (see Figures 7, 8 and 12). Note that these two designs provide the best performance of all the designs at the shallower elevation angles ($< 10^{-9}$ at $6^\circ < \theta < 9^\circ$). No doubt that the greater

number of baffles, in the case of OBD5 (10 compared with 5 for the other designs), or the wider baffle openings in the case of OBD4 creates a higher probability that an entering photon will get trapped within one or more of the openings. Also note that OBD2 surpasses the performance of OBD3 because it has deeper openings, which also keeps photons trapped longer. The upshot of these results are all rather intuitive, and the following summarizes what design attributes give the highest light suppression:

- Greater number of baffle openings within a given space offer a higher probability of initially trapping a photon;
- Deeper baffle openings force a greater number of internal bounces within an opening;
- Flat surfaces between openings reflect photons back towards the entrance (and away from the detector).

With a light suppression of $<10^{-9}$ using the high reflectivity value of 0.9 for OBD4 and OBD5, this equates to a light suppression of $<10^{-197}$ (or effectively 0) with a lower reflectivity of 0.1 assuming that the photons entering the spherical deflection plate section all have input elevation angles between 6° and 9° , and that they all start at the center of the instrument! Of course, this will not always be the case; hence a full trace of the entire instrument is necessary. However, we have gained much insight into the performance of the OBD design with this initial look at their light suppression performance.

In the next section, I will report on the performance of OBDs1-5 with photons entering from the outside of the instrument. This will tell us what the overall light suppression is for the various OBD designs, keeping with the single top hat baffle design as mentioned above.

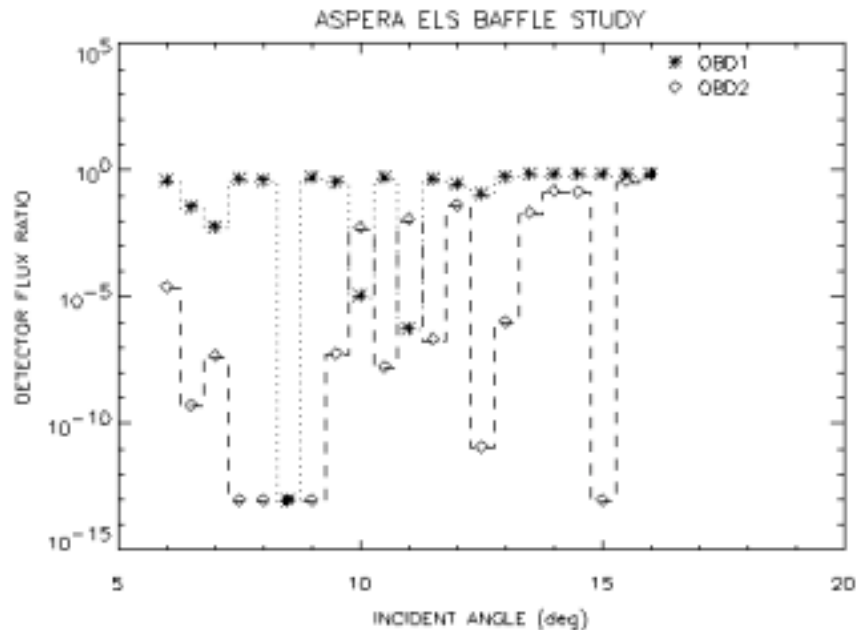


Figure 5. Plot showing the normalized flux reaching the detector (detector flux ratio) from a radiant spot located in the center of the top hat as a function of incident angle measured from the horizontal axis (see Figure 1) for OBD1 and OBD2. Note that OBD2 has lower detector flux ratios at most incident angles than OBD1 due to its flat faceted surfaces.

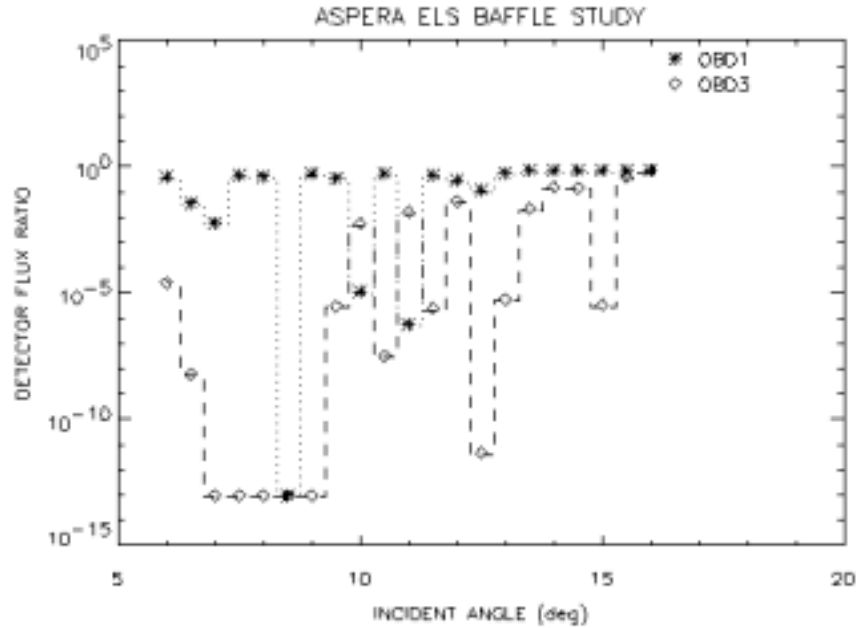


Figure 6. Same as in Figure 5 with comparison between OBD1 and OBD3. Again, note that OBD3 has lower detector flux ratios than OBD1 at nearly all incident angles.

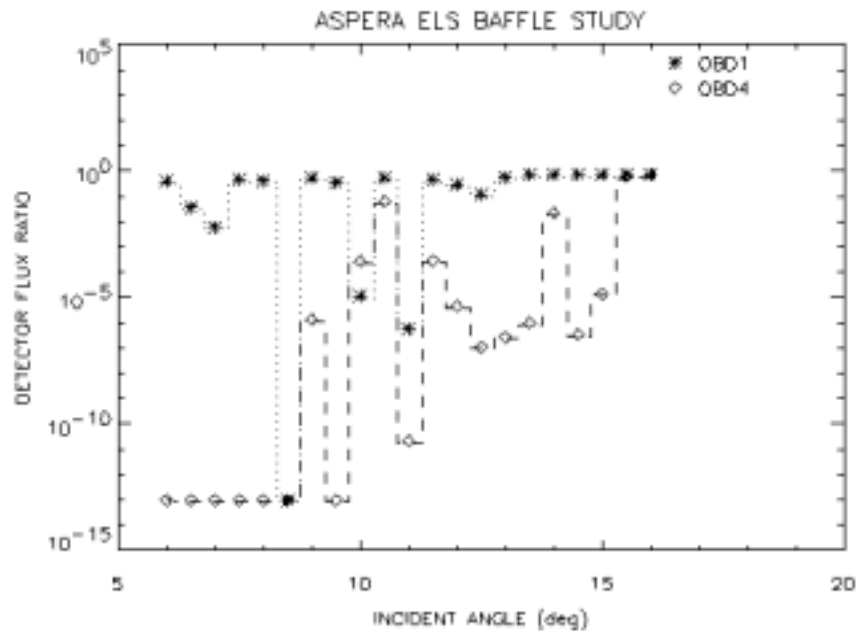


Figure 7. Same as in Figure 5 with comparison between OBD1 and OBD4. Again, note that OBD4 has lower detector flux ratios than OBD1 at nearly all incident angles.

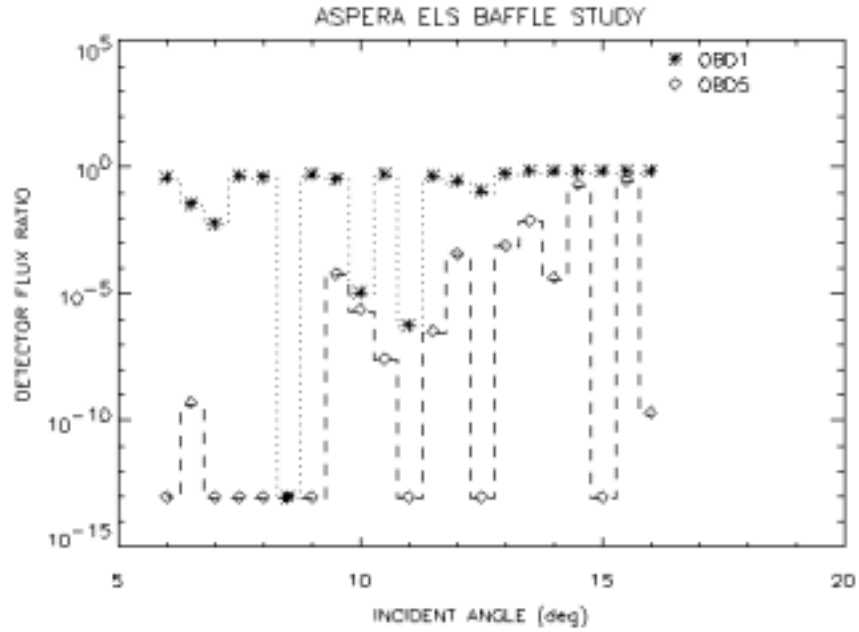


Figure 8. Same as in Figure 5 with comparison between OBD1 and OBD5. Again, note that OBD5 has lower detector flux ratios than OBD1 at all incident angles.

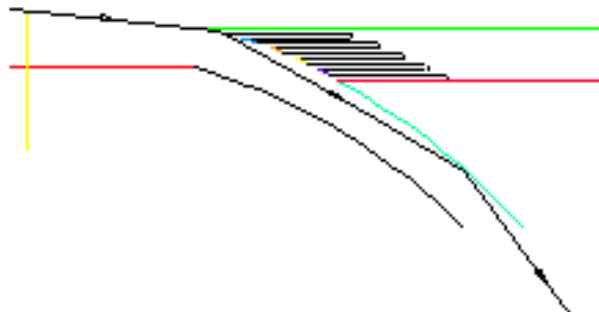


Figure 9. Trace of one ray through OBD1 showing a reflection off the baffle edge with the ray deflected downwards towards the detector.

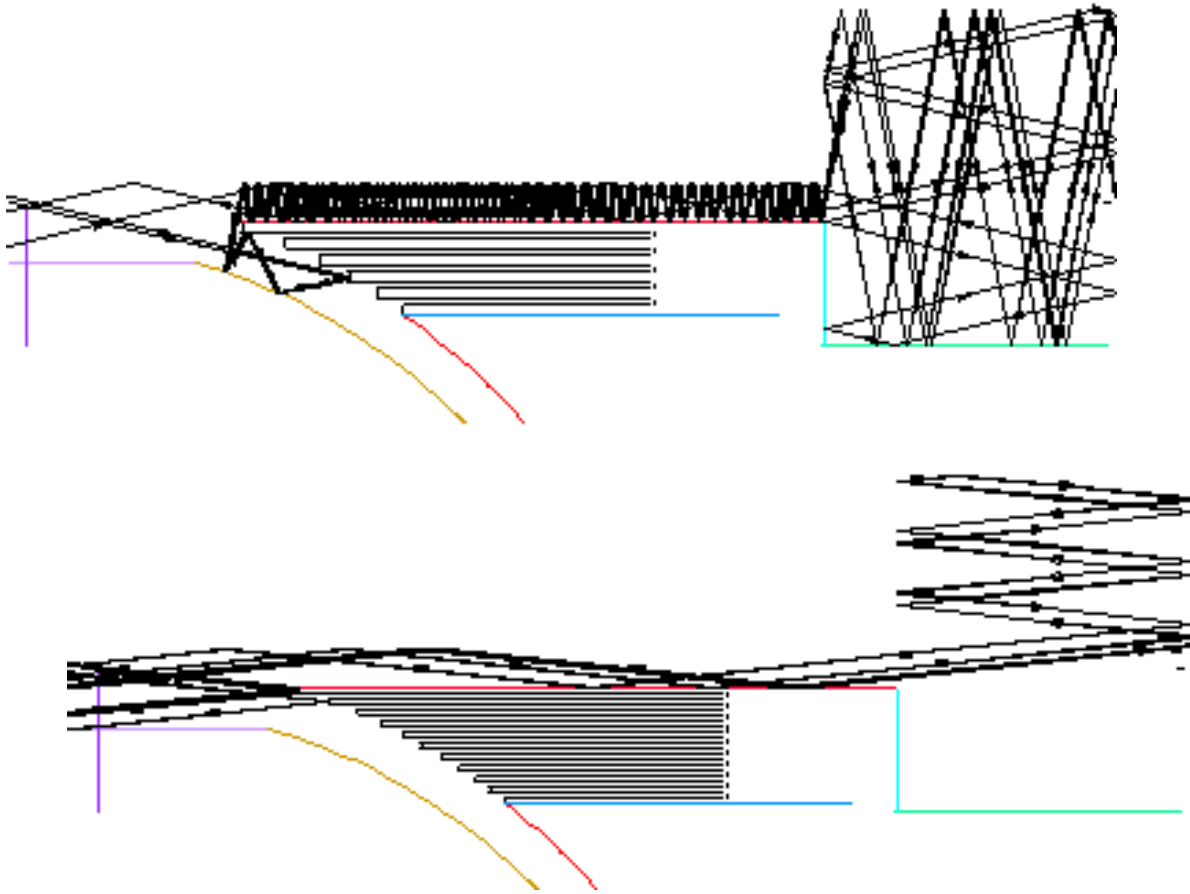


Figure 10. Trace of a handful of rays through OBD2 (top) and OBD5 (bottom) showing reflections off the flat baffle edges back towards the outer opening to the instrument. Note how the rays are reflected back towards the main top hat baffles and trapped.

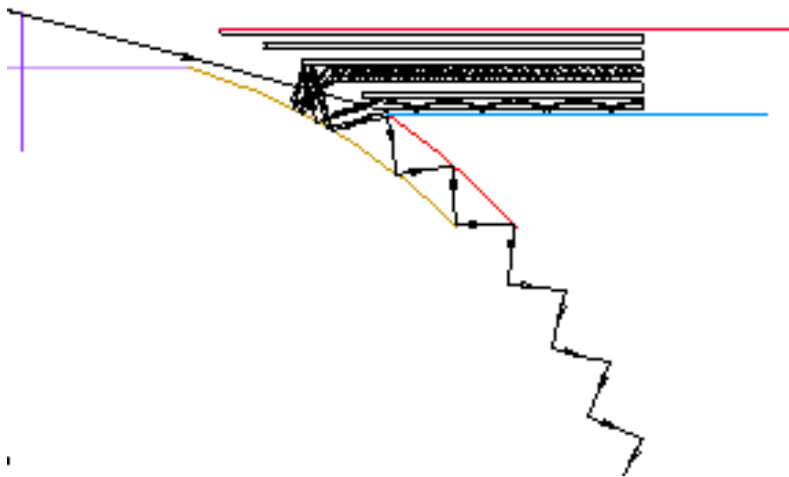


Figure 11. Trace of a single ray through OBD4 showing how the ray is trapped within two baffle openings before it eventually escapes and heads down towards the detector. Note however that by the time the ray reaches the detector, it has made over 100 reflections.

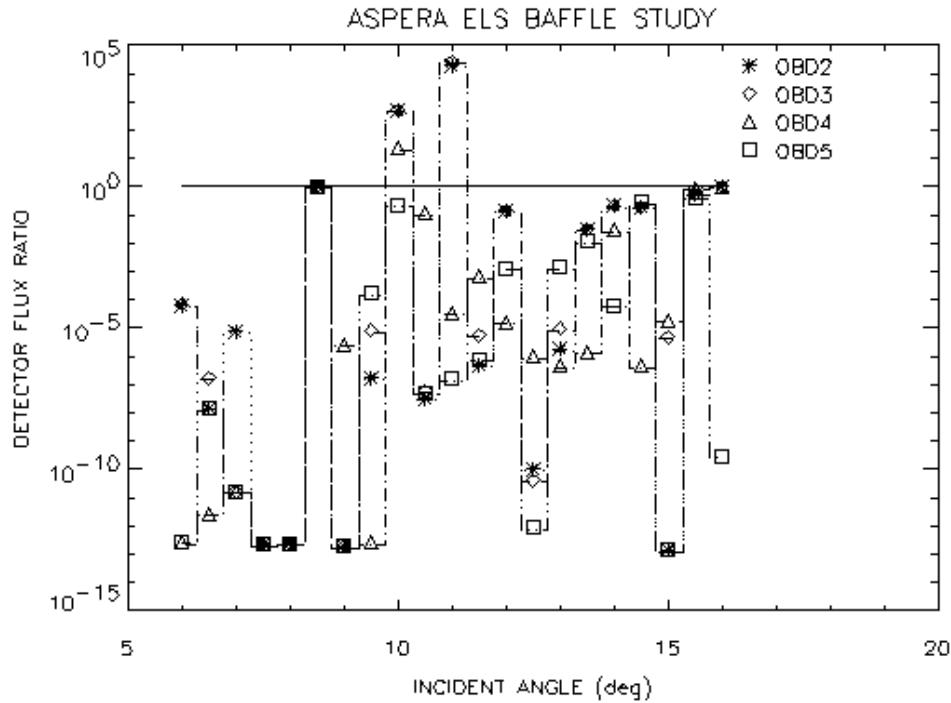


Figure 12. Ratio of flux ratios reaching detector for OBDs2-4 to that of OBD1. Note that the ratio is always < 1 for OBD5 making it the best overall performer in suppressing rays emanating from the center of the top hat region.

III. ELS UV LIGHT SUPPRESSION RESULTS

A. Ray Trace Runs

Collimated light rays were traced through the entire instrument emanating from a rectangular grid source placed outside the instrument with dimensions of 0.14" x 5" that filled the entrance aperture of the instrument. The elevation angle of the rays entering the instrument was varied between -10° and $+10^\circ$ in 1° increments (see Figure 13); the azimuthal angle of all rays was fixed at 0° . The source grid was composed of a total of 10^5 rays arranged with 1000 rays along the x -axis, and 100 rays along the y -axis. Each of the five OBD designs was traced with this input source, and the number and intensity of the rays reaching the detector was recorded at each elevation angle using three values for the reflectivity of the interior surfaces: 0.9, 0.5, and 0.1 (assuming specular reflections at each surface). Figures 14-18 show the results of these runs for each OBD design. The dashed line at a flux ratio of 10^{-10} in each of these plots is the desired maximum flux ratio to keep the detector background rate from Solar H-Ly α below a few counts per second. Table II summarizes the ray trace results in tabular form.

TABLE II. UV Suppression Results							
Baffle Design	Detector Flux Ratio (flux that reaches detector assuming total flux entering instrument is 1)						Reflectivity ⁽²⁾ ($\Phi_r < 10^{-10}$)
	$R^{(1)} = 0.9$		$R^{(1)} = 0.5$		$R^{(1)} = 0.1$		
	Minimum	Maximum ⁽³⁾	Minimum	Maximum ⁽³⁾	Minimum	Maximum ⁽³⁾	
OBD1	< 1.0E-20	1.4E-03 (-2°)	< 1.0E-50	6.5E-05 (-2°)	< 1.0E-50	8.1E-08 (-2°)	< 0.02
OBD2	< 1.0E-20	3.2E-04 (-2°)	< 1.0E-50	9.8E-07 (-2°)	< 1.0E-50	1.2E-12 (-2°)	< 0.17
OBD3	< 1.0E-20	2.9E-04 (-2°)	< 1.0E-50	8.6E-07 (-2°)	< 1.0E-50	1.2E-12 (-2°)	< 0.18
OBD4	< 1.0E-20	6.2E-05 (-2°)	< 1.0E-50	1.9E-07 (-2°)	< 1.0E-50	2.1E-13 (-2°)	< 0.21
OBD5	< 1.0E-20	6.4E-05 (3°)	< 1.0E-50	2.4E-07 (3°)	< 1.0E-50	4.2E-13 (3°)	< 0.20

(1) Surface reflectivity values.
 (2) Surface reflectivity value to achieve a detector flux ratio (Φ_r) of $< 10^{-10}$ at all input elevation angles.
 (3) Maximum Φ_r at the elevation angle shown in parentheses.

B. Discussion

The results in Table II (and Figures 14-18) clearly show that OBD1 has the poorest light suppression performance as was predicted based on the earlier outer plate baffle results (see § II.B). Somewhat surprisingly, however, OBD4 showed slightly better light suppression than OBD5. In this case, larger baffle openings seem to better trap incoming rays than a greater number of narrower ones.

The minimum flux reaching the detector (we indicate this here as the detector flux ratio, Φ_r , or the total flux reaching the detector with a total input flux to the instrument of one) is $<10^{-20}$ for all OBD designs (with surface reflectivity values, R , of ≤ 0.9). Note, however, that all OBD designs have Φ_r values that exceed the desired 10^{-10} value for $R = 0.9$ and 0.5 (and in fact OBD1 exceeds this value for $R = 0.1$). Also note that most vulnerable input elevation angle is -2° for all but OBD5.

To guarantee that $\Phi_r < 10^{-10}$ at all elevation angles, R must be no larger than that tabulated in column 8 of Table II. With OBDs2-5, the maximum R is ~ 0.2 ; OBD1 requires an $R < 0.02$! Clearly, OBDs2-5 show superior light suppression qualities over OBD1. OBDs2-5 on the other hand show only slight light suppression performance differences, with OBD4 holding the edge.

C. Recommendations

If $R < 0.1$ for CuO at H-Ly α , then any one of the four OBDs2-5 is an adequate design for the ELS instrument. To insure adequate light suppression, I recommend OBD4 in combination with an internal coating with a surface reflectivity of <0.1 at H-Ly α (1216 Å). In addition, all joints within the instrument housing must be made light tight. To suppress photoelectrons generated inside the instrument, a repeller grid biased slightly negative above the MCP detector surface should be included.

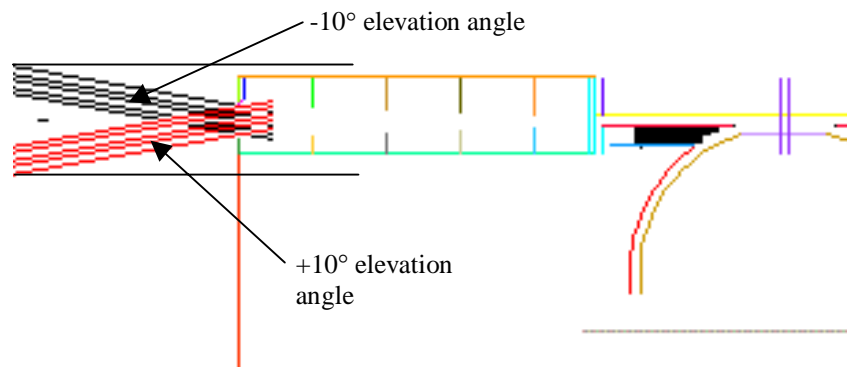


Figure 13. Schematic showing how the elevation angles for the input grid of rays are defined for the ray traces.

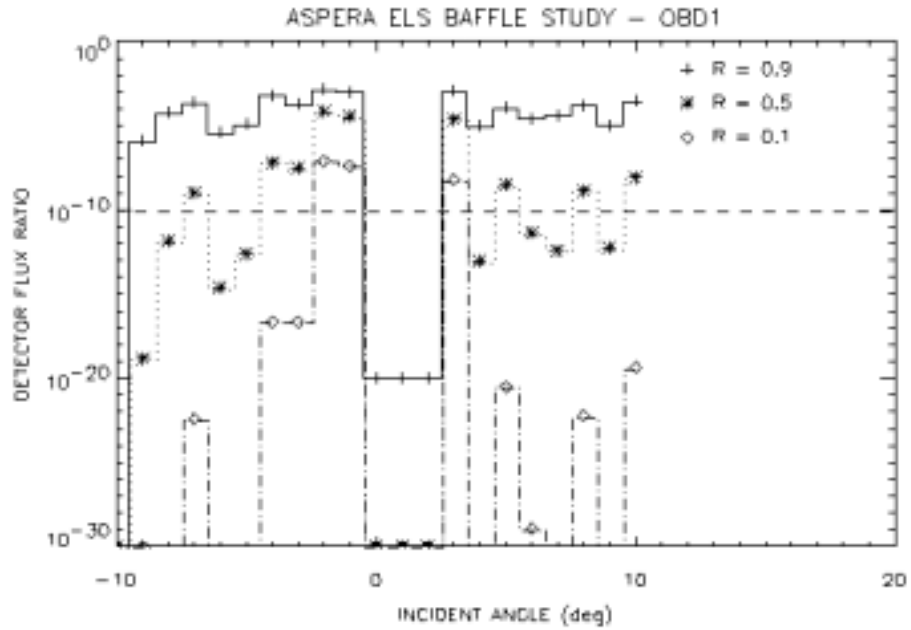


Figure 14. Detector flux ratio plotted against the incident elevation angle of the incident rays entering the instrument (see figure 13) for OBD1 at three values of the surface reflectivity: 0.9, 0.5, and 0.1. The dashed horizontal line at 10^{-10} is the maximum desired flux ratio to maintain a low (i.e. $1-2 \text{ s}^{-1}$) background rate caused by UV light.

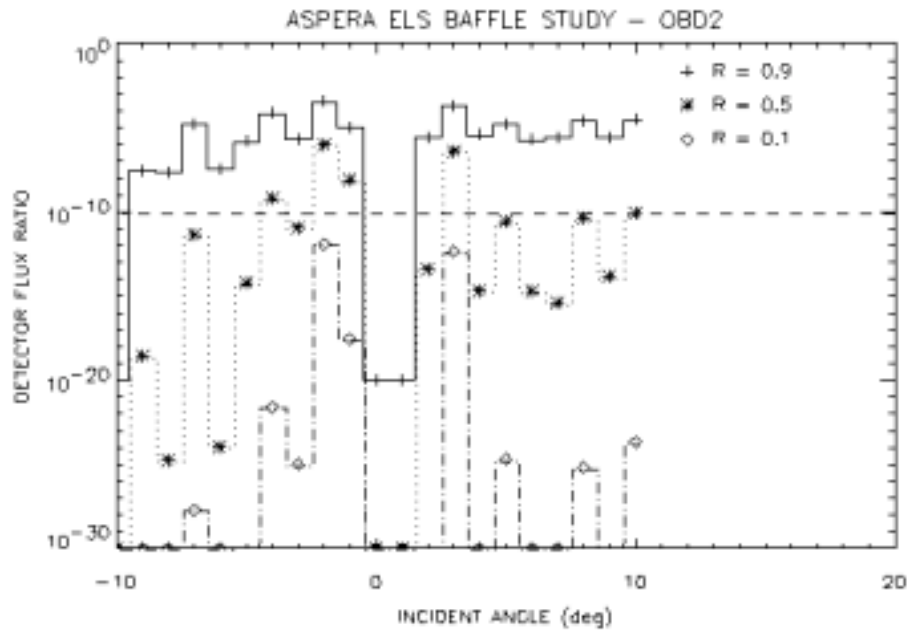


Figure 15. Same as Figure 14 with OBD2.

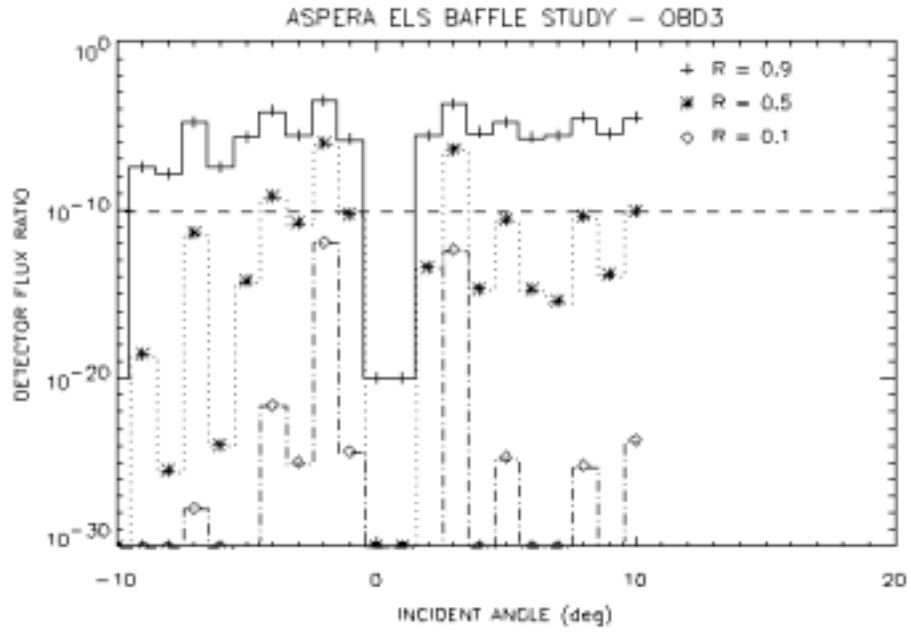


Figure 16. Same as Figure 14 with OBD3.

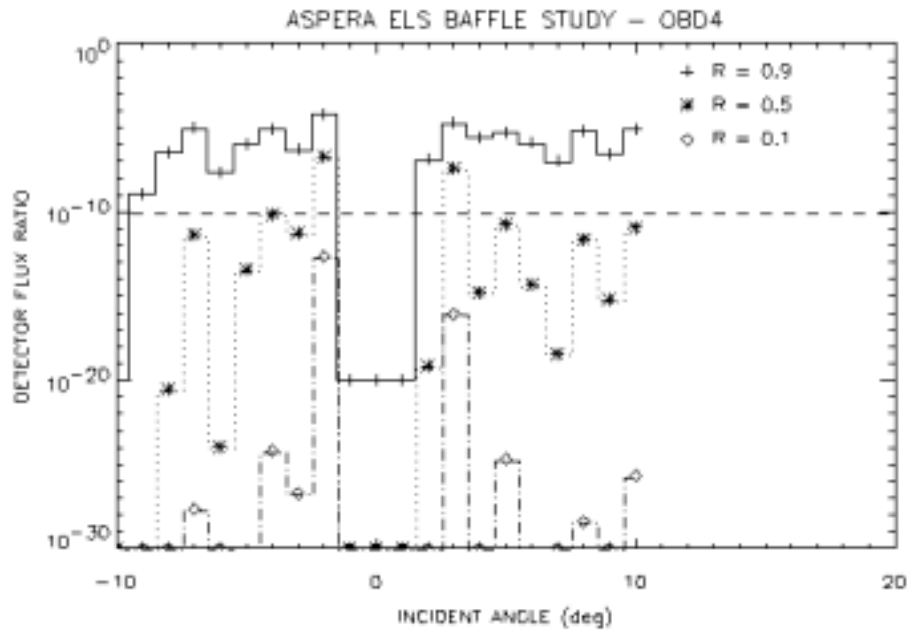


Figure 17. Same as Figure 14 with OBD4.

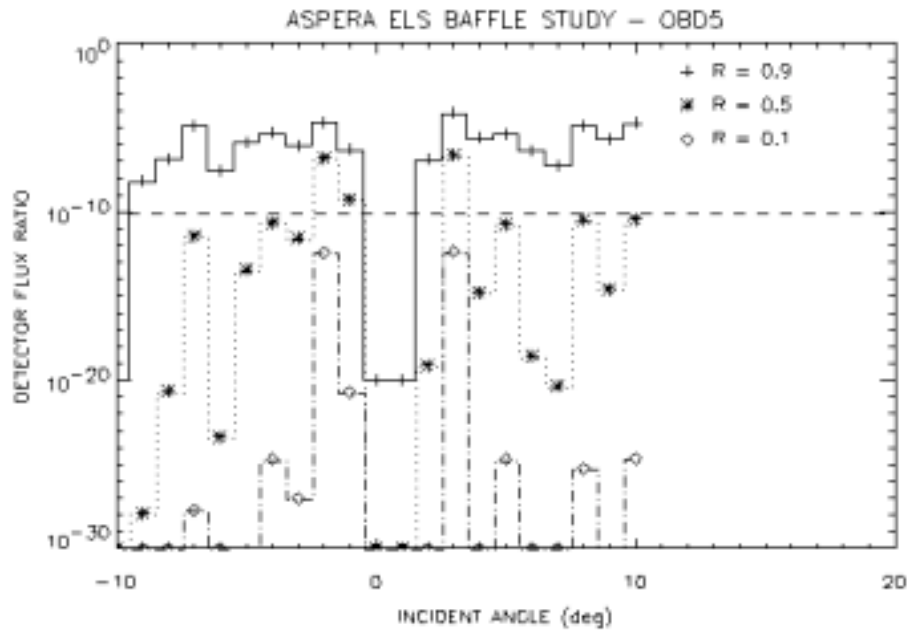


Figure 18. Same as Figure 14 with OBD5.